Available online at www.garmian.edu.krd

Passer Journal

Passer

Passer 5 (Issue 1) (2023) 144-152

http://passer.garmian.edu.krd/

Fault Detection of Underground Cable Using FFT in Kurdistan Area

Azad Hussein Zubair[1*], Kamal Sheikh Younis[1]

[1]*Electrical Department, College of Engineering, Salahaddin University, Erbil, Kurdistan Region, Iraq*

Received 06 March 2023; revised 28 March 2023;
accepted 6 April 2023; available online 08 April 2023

DOI: 10.24271/PSR.2023.388610.1275

ABSTRACT

The modeling and computation of a single line-to-ground fault of the distribution for underground cables have distinct characteristics compared to circuits with standard voltage and current waves. This work presents a mathematical analysis and modeling of 3-phase, open circuit, and single line-to-ground cables for the Azadi distribution substation lines. The feature of increased harmonic amplification of individual frequencies is that detecting single-phase faults can be determined using fast Fourier transform (FFT) analysis. The validity of chain equivalent schemas with constant parameters for a single frequency makes it possible to investigate the nature of wave process through the discrete selection of parameters. The proposed method selected several cases of wave cycles for both voltage and current. Also, during the analysis, several starting times before and after the fault is chosen to determine the total wave distortion. The results show that the best analysis that could detect the faults is three cycles. The FFT of three cycles has the maximum values of distortion in most of the cases. All the FFT is done using the MATLAB Simulink program.

Keywords: Fault detection, Fast Fourier Transform, Single-Line-Ground Fault, Underground Cable.

1. Introduction

The most probable fault for power systems is the distribution lines which, are the majority of those faults are single-line-to-ground faults[1]. Power distribution lines have a significant role in the electrical power continuity from sources to users. On the other hand, the practical results of the high impedance non-effective grounding system are higher reliability and security than the effective grounding system[2]. According to the low value of the single line-to-ground fault current in the high-impedance grounding system, the line-to-line voltage remains constant, and the supply of electric power could be reminding for a long[1, 3, 4]. The importance of the earlier detection of the fault increases in underground cables. When the system's insulation fails at any point, a fault is described as a collection of unfavorable but unavoidable events that may momentarily affect the stable state of the power system.

Several methods have been done to study the types, currents, voltage, frequency, location and harmonics of the faults[5-7]. For example, Mahanty and Gupta[8] discovered that the devised approach requires only current samples following the transmission line fault at one side. Discretized wavelets transform (DWT) was proposed by Ashok et al. [9] for the transmission system problems. The authors provided a method for safeguarding the 3-terminal transmission system utilizing DWT for fault classification. A solution for 3-terminal protection issue of TL standard using DWT of fault classification was introduced by Kumar and Sagar[10]. On 400 kV, 300 km transmission line models intended for various single phase-to-ground faults, simulation studies are conducted using electromagnetic transients, direct current and computer-aided design software for power systems[11]. While Prasad and Edward[12] opinion that the currents at one end of the overhead wire with the aid of DWT to construct a novel solution. The fault topic is not an exception, Komen et al.[13] used Fuzzy logic to develop an approach for fault analysis using current samples. Only one end of the 3-phase current samples was deemed to have accomplished the fault categorization using this method. Prasad et al.[14] used fuzzy logic and created a method to identify line-to-ground faults. Also the lightning strikes that hit nearby above lines impact underground cables. Opening and closing switching devices at various points in the cable system as well as electrical problems both, could be caused to switching overvoltages[5].

The achievements for the signal waves, and distortion during the fault led to an increase in the spot on the fault signal analysis of power systems, especially the overhead transmission lines[5, 7]. However, the correct number of waves that must be selected still needs to be carefully selected to get the optimal device sensitivity and faster decision. The optical spectrum of a given

* Corresponding author
E-mail address: azdzuber76@gmail.com (Instructor).
Peer-reviewed under the responsibility of the University of Garmian.

surface area can often be measured from a stationary point by standard commercial spectrometers or spectrophotometers [15].

As a particular case, this work introduces a study case of the Azadi substation transmission system in the Kurdistan area of Iraq. A calculation of the frequency characteristics of the frequency via the voltage and currents in the healthy and faulty phases. The work examines five cases for cycle number and five starting times for the wave analysis. This FFT is done for the voltage and healthy and faulty currents using MATLAB. The high values of distortion increase the insurance of fault detection. The comparison between the FFT for all of the results suggested that assuming the analysis of the three cycles can discover the fault earlier. All that is done after a mathematical introduction for the line characteristics model.

Table 1: The symbol description used in the paper.

Symbol	Descriptions
$C_{\grave{M}}$	Capacitance star
C_M	Capacitance between conductors
C_O	The total capacitance of the line
I_g	Ground fault current
I_o	Zero component current
L_O	The total inductance of the line
R_N	The neutral grounding resistance
R_T	Resistance of the transformer
R_g	Ground arc faults resistance
R_n	Grounded neutral resistance
T_a	Time constant
U_{ph}	Phase voltage
U_{rated}	Rated voltage
X_T	Reactance of the transformer
c_{on}	Connected to the ground for the nth lines by the total phase capacitance
e_{kh}	Input voltage vector
e_{mh}	Output voltage vector
i_k	The modal current into the end-node vector
i_m	The modal current into the end-node vector
l_n	Nth line length
nx_k	nth component Input impedance
nx_n	nth component output impedance
v_k	Input voltage
v_m	Output voltage
x_N	Output impedance
x_k	Input impedance
τ_i	Traveling time constant
C	Capacitance between conductors and ground
FC	Frequency characteristics
FFT	Fast Fourier transform
N	Number of line
THD	Total harmonic distortion
X	Load reactance
Zc	Characteristic impedance in modal quantities
β	Phase change coefficient
ω	Frequency of the current

2. Mathematical analysis

Electrical machine frequency characteristics (FCs) are actively employed to studies the modes of operation and spot emerging flaws. We will identify which factors, including synchronous and asynchronous machines, transformers, and autotransformers, should be considered by the power systems before moving forward with (FC) power transmission.

There are further prospects for using (FCs) because it is also conceivable to use the same voltage transformers on the switchgear buses and the high side of the consumer substation. Due to those mentioned above, data on the zero-sequence component of currents and voltages in addition to phase voltages and phase currents. The positive and negative sequence components may now be separated using modern microprocessor devices, which can once more be utilized to pinpoint the location of line damage.

Mathematical model of symmetrical switching of the high harmonics source

In this instance, let us assume that the conductors of the underground cables are positioned symmetrically. The three-phase power radial distribution schematic diagram is shown in Figure 1.

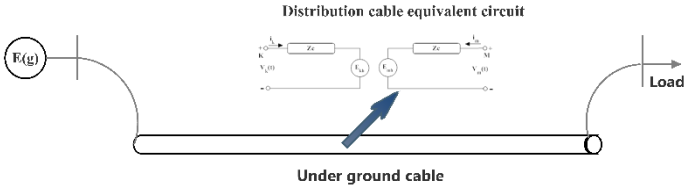

Figure 1: Radial cable distribution system scheme[5].

Taking into account the equivalent circuit that is shown. Moreover, when operating at high frequencies, we neglected the resistance's impact on the frequency corresponding to the maximum voltage at the supply's end.

It is clear from Figure 2 of the equivalent circuit that the highest voltage V_2 will match the maximum voltage V_z that is measured on the output side. The latter situation is crucial because it enables low-voltage measuring circuits in step-down substations without needing a high-voltage measuring transformer.

The voltage source vectors for both input and output are updated

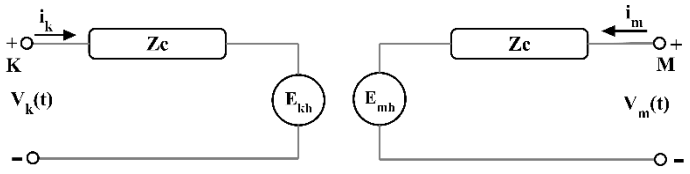

Figure 2: Equivalent circuit of underground distribution cable[5].

with the time according to equations (1) and (2)[5].

$$\left[e_{kh(t)}\right] = [z_c][i_m(t-\tau_i)] + [v_m(t-\tau_i)] \quad (1)$$

$$[e_{mh}(t)] = [z_c][i_k(t-\tau_i)] + [v_k(t-\tau_i)] \quad (2)$$

Where:

z_c is the characteristic impedance in modal quantities

$e_{mh}(t)$, $e_{kh}(t)$ are history voltage sources of the ideal line section

τ_i *is* traveling time

$v_k\ (t)$, $v_m\ (t)$ are the input and output voltage vectors.

$i_k\ (t)$, $i_m\ (t)$ are the input and output currents vector for a line without losses[16].

$$Z_c = \sqrt{L_0/C_0} \qquad \omega\beta = \sqrt{\omega L_0 \omega C_0} = \omega\sqrt{L_0 C_0} = \omega\beta \tag{3}$$

The frequency characteristics of the electrical transmission could be as in (4) [16]

$$\dot{W}_2 = \frac{\dot{V}_2}{\dot{E}} = \dot{W}_2 = \frac{1}{\left(1+\frac{X_K}{X_N}\right)\cos(n\beta l) - \left(\frac{nx_k}{z_c} - \frac{z_c}{nx_n}\right)\sin(n\beta l)} \tag{4}$$

If we neglect the internal impedance of the source. Then formula (4) is transformed into the following[16].

$$t_g(n\beta l) = -\frac{nx_n}{z_c} \tag{5}$$

The mathematical model of single phase-to-ground fault for the underground cable with distributed parameters[16].

$$T_A = \frac{3R_g R_n C}{R_g + R_N} \tag{6}$$

Based on equation (6), decreases in time constant Ta, the ground arc fault's resistance decreases Rg. Therefore, it is thought $Rg \to \infty$ it raises the

$$T_a = \frac{3R_N C}{1 + R_N/R_g} = 3R_N C \tag{7}$$

At the same time, the formulae below stipulate that such an extinguishing must occur within the main's first half period[16].

$$R_N = \frac{T_a}{3c} = \frac{0.01}{3\times3\times C} = \frac{1}{900C} \tag{8}$$

Based on given by:

$$\frac{C_M}{C} = \frac{1}{3} \qquad for\ the\ cable \tag{9}$$

$C'_m = 3Cm$. Moreover, the total capacitance is [16].

$$C_0 = C + C'_m = C+3\ C_m \tag{10}$$

Taking into account (9):

$$C_0 = C + 3C_m = C + \frac{3}{3}\ C = 2C \tag{11}$$

The total cable capacitance could be estimated to the ground

$$C = \frac{1}{2}\ C_0 \tag{12}$$

$$C = \frac{5}{8} C_0 \tag{13}$$

the four cases of the standard cables in Kurdistan are given in Table 2. the data is obtained from the ministry of electricity of the Kurdistan region.

Table 2: Cables Parameter details.

No.	Types	R ohm/km	L mH/km	C µf/km
1	3*185/25	0.0991	0.319	0.243
2	3*240/25	0.0754	0.304	0.273
3	3*300/25	0.0601	0.295	0.296
4	3*400/25	0.0470	0.284	0.331

1-

Zc= $\sqrt{L_0/C_0} = \sqrt{0.319/0.243}$ = 1.145 ohm

$\beta = \sqrt{L_0 C_0}$ =$\sqrt{0.319 * 0.243}$ =0.278

cm =$\frac{1}{3}$c for cables cm = $\frac{1}{3}$0.243 =0.081 µf

RN=$\frac{1}{900C}$ =$\frac{1}{900*0.243}$ =4.5m ohm = 0.045 ohm

2-

Zc= $\sqrt{L_0/C_0} = \sqrt{0.304/0.273}$ = 1.055 ohm

$\beta = \sqrt{L_0 C_0}$ =$\sqrt{0.304 * 0.273}$ =0.288

cm =$\frac{1}{3}$c for cables cm = $\frac{1}{3}$0.273 =0.091 µf

RN=$\frac{1}{900C}$ =$\frac{1}{900*0.273}$ =0.407m ohm = 0.00407 ohm

3-

Zc= $\sqrt{L_0/C_0} = \sqrt{0.295/0.296}$ = 0.998 ohm

$\beta = \sqrt{L_0 C_0}$ =$\sqrt{0.295 * 0.296}$ =0.295

cm =$\frac{1}{3}$c for cables cm = $\frac{1}{3}$0.296 =0.098 µf

RN = $\frac{1}{900C}$ =$\frac{1}{900*0.296}$ = 0.00375 ohm

4-

$Zc=\sqrt{L_0/C_0}=\sqrt{0.284/0.331}$ = 0.92628 ohm

$\beta = \sqrt{L_0 C_0}$ $=\sqrt{0.284 * 0.331}$ =0.3066

cm $=\frac{1}{3}$c for cables cm $=\frac{1}{3}0.331$ =0.1103 µf

RN$=\frac{1}{900C}$ $=\frac{1}{900*0.331}$ =3.3568$m$ohm=0.033568 ohm

The ratios (11) and (12), which demonstrate how different the line's capacity is from its entire (full) capacity, are of utmost significance. When analyzing an electrical network project that was planned, the ground fault current Ig should be calculated using the same expressions as a starting point according to:

$$I_g = \sqrt{3}\, U_{rated} \sum_{n=1}^{N} \omega C_{on} l_n \quad (13)$$

N is the number of lines that the common bus supplies, ln is the n[th] line's length, and C_{0n} is connected to ground for the n[th] line by the total phase capacitance.

$$I_g = 3I_0 = U_{ph}\left\{j3\omega C + \frac{3}{3R_T + jX_T}\right\} \quad (14)$$

3. Results and dissections

The parameters in the first row of Table 2 are used in this work.

The system modeling is shown in Fig.3. The simulation model consists of a 3-phase, 11kV source, network transformer, and overhead transmission.

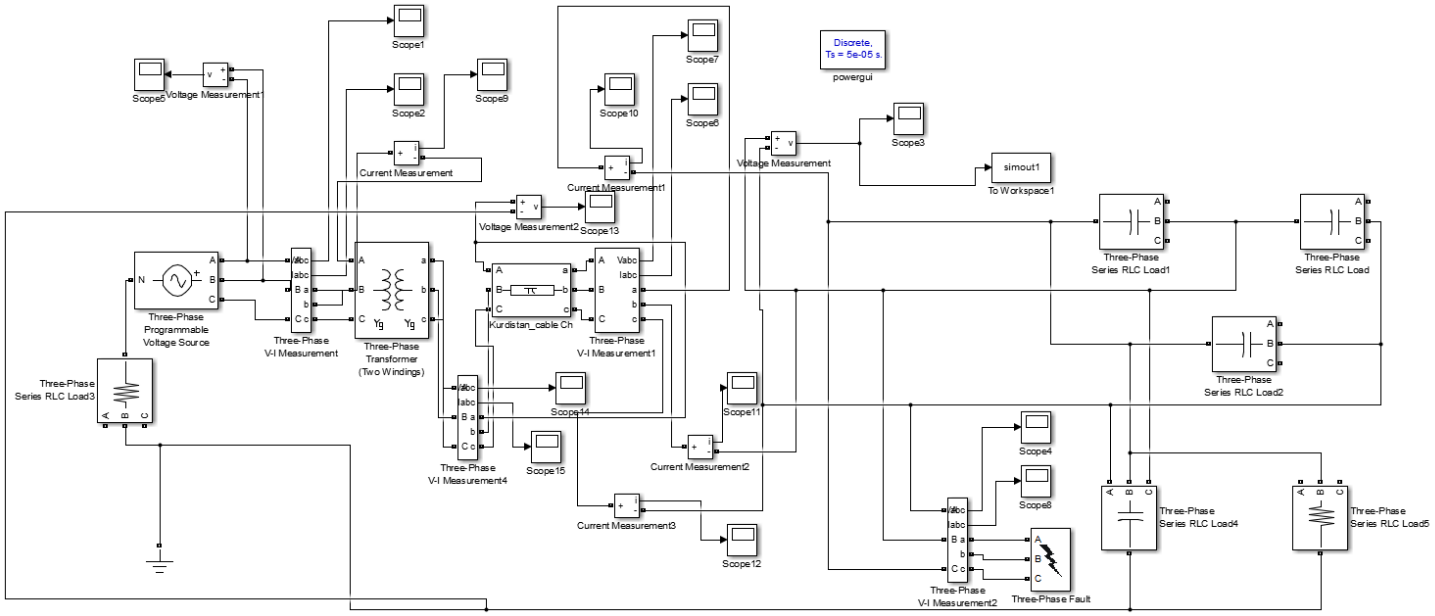

Figure 3: Simulation diagram of the single line to ground fault system model.

In this work, fast Fourier transforms (FFT) analysis for a 20 km, Kurdistan system of underground cable line is done to study the effect of fault on the high capacitance lines. The analysis involves the three-phase voltage and current of healthy and faulty lines. A single phase to ground fault is selected to examine the Simulink system. Figure 4. Presents the FFT analysis for the voltage and current for three cycles without fault. The authors used the FFT analysis of MATLAB to analyze the components of the signal that companions to the primary frequency. Also, FFT analysis, gives the total signal distortion that may happen during the power system operation and control.

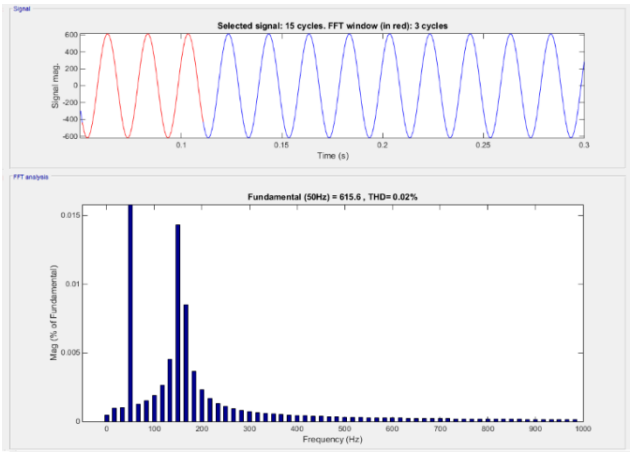

a

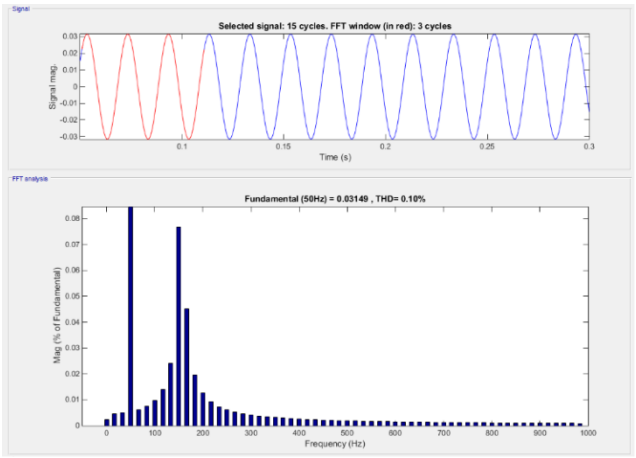

b

Figure 4: FFT case of 3cycles, starting time 0.051s, and without fault (a) voltage analysis (b) phase-1 current analysis.

The previously selected analysis is used to be the base of the comparison between the voltage and currents for the healthy and the faulty line. Figure 5. Table 3 represents the voltage FFT for specific cases of the voltage cycles and different starting times. The three cases of the started times are selected to present the Fourier analysis before, during, and past fault timing.

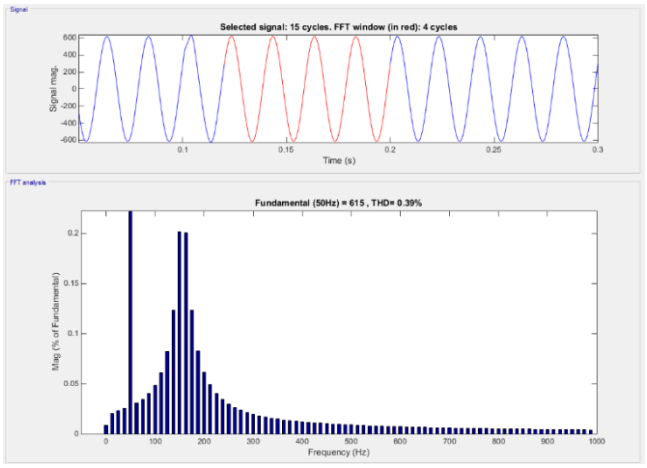

a

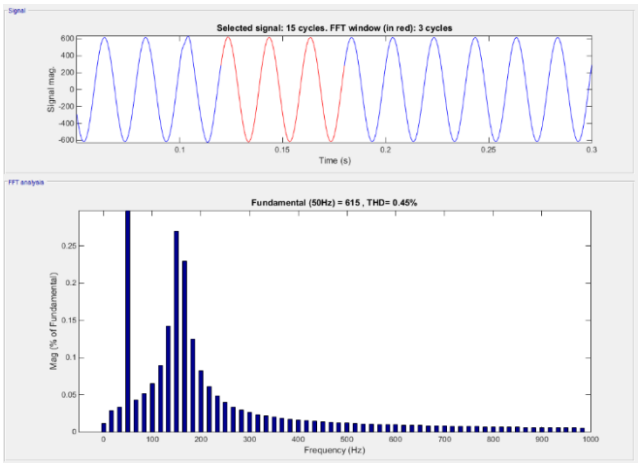

b

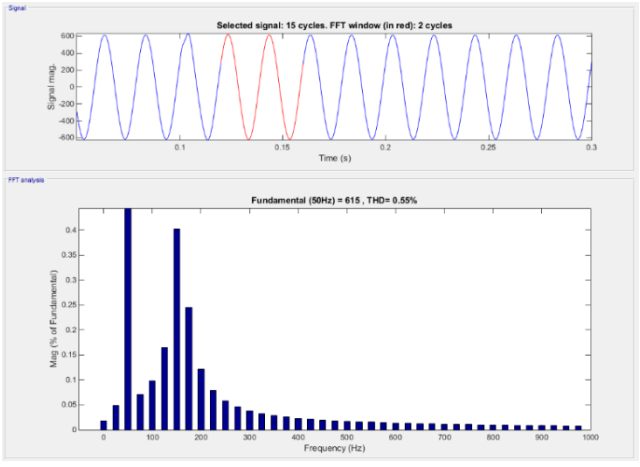

c

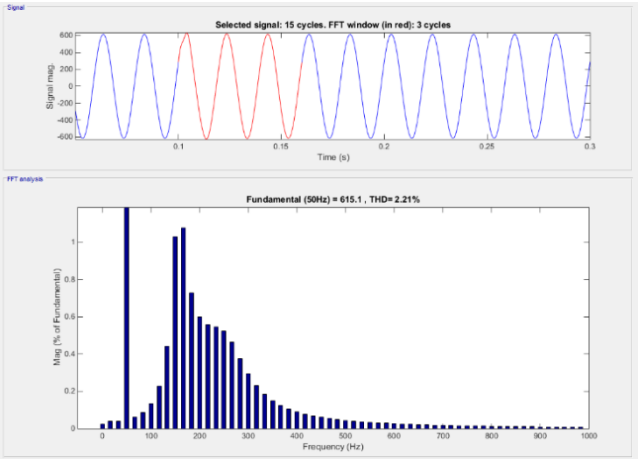

d

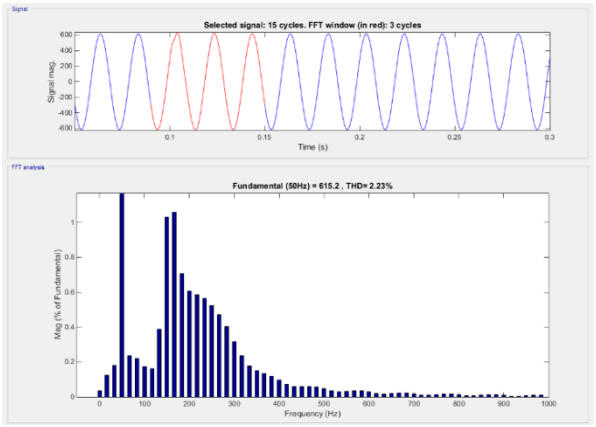

e

Figure 5: FFT voltage analysis during a continuous fault (a) case of 4 cycles, starting time 0.12s (b) case of 3 cycles, starting time 0.12s (c) case of 2 cycles, starting time 0.12s (d) case of 3 cycles, starting time 0.1s (e) case of 3 cycles, starting time 0.09s.

Regarding Figure 5., it can be noticed that the total harmonic distortion (THD) and the high harmonic value compared to the fundamental frequency. Table 4 represents the THD compression for all cases done in this work via the voltage distortion.

The current analysis was also studied to analyze the system. Phase-3, which is the healthy line, is studied to have information on the frequencies accompanying the fundamental frequencies. Figure 6. illustrates the phase-3 analysis.

Table 3: Voltage THD % values.

Starting time	With fault					Without fault				
	1	2	3	4	5	1	2	3	4	5
0.12	0.76	0.55	0.45	0.39	0.35	0.01	0.02	0.02	0.02	0.01
0.1	3.75	2.71	2.21	1.92	1.71					
0.09	3.48	2.72	2.23	1.93	1.73					
0.075	0.01	2.58	2.23	1.94	1.74					
0.051	0.03	0.02	2.04	1.94	1.75					

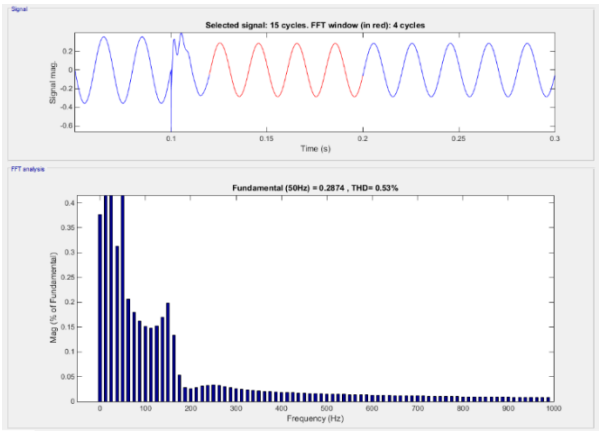

a

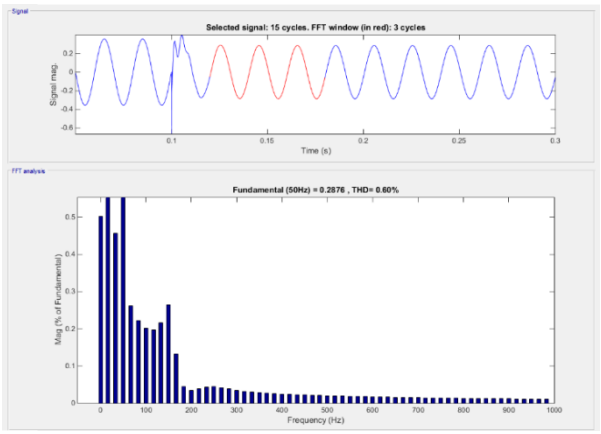

b

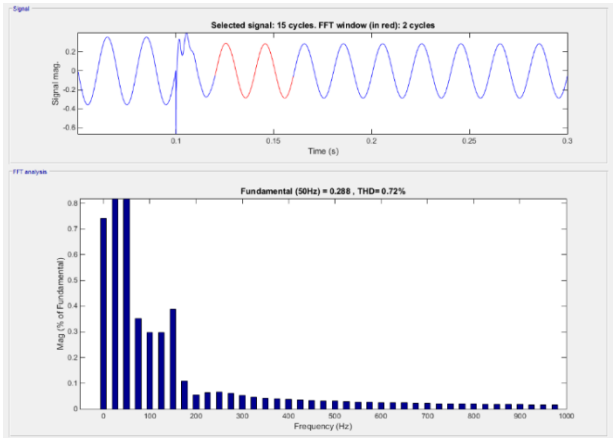

c

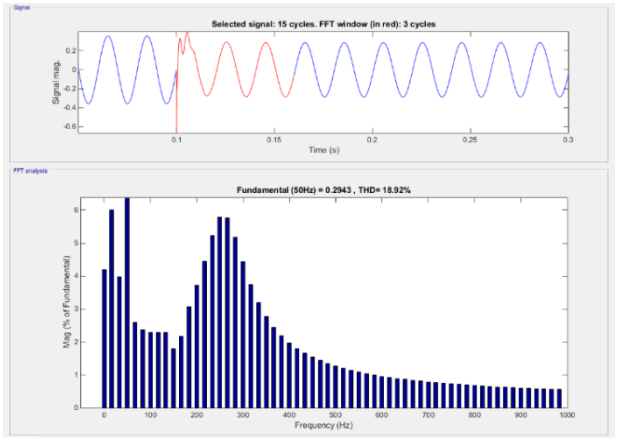

d

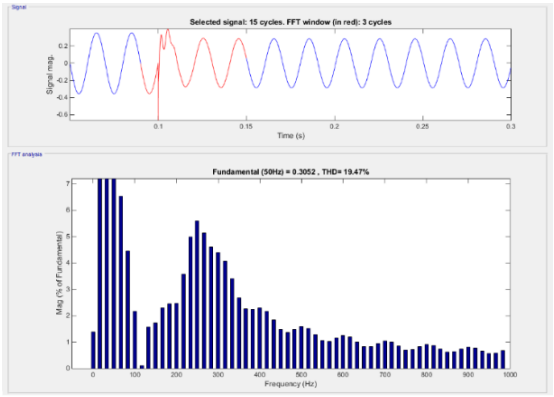

e

Figure 6: FFT healthy phase current analysis during a continuous fault (a) case of 4 cycles, starting time 0.12s (b) case of 3 cycles, starting time 0.12s (c) case of 2 cycles, starting time 0.12s (d) case of 3 cycles, starting time 0.1s (c) case of 3 cycles, starting time 0.09s.

Table 5. represents the THD compression for all cases done in this work via the healthy phase distortion.

The current analysis was also studied to analyze the system. Phase-1, which is the faulty line, is studied to have the information on the frequencies that accompany fundamental frequencies. Figure 7. illustrates the phase-1 analysis.

Table 4: Phase-3 current THD% values.

Starting time	With fault					Without fault				
	1	2	3	4	5	1	2	3	4	5
0.12	0.87	0.72	0.60	0.53	0.48	0.15	0.12	0.10	0.09	0.08
0.1	30.95	22.81	18.92	16.52	14.85					
0.09	27.54	22.69	19.47	17.29	15.70					
0.075	0.00	21.57	19.54	17.81	16.51					
0.0501	0.00	0.00	15.89	16.23	15.96					

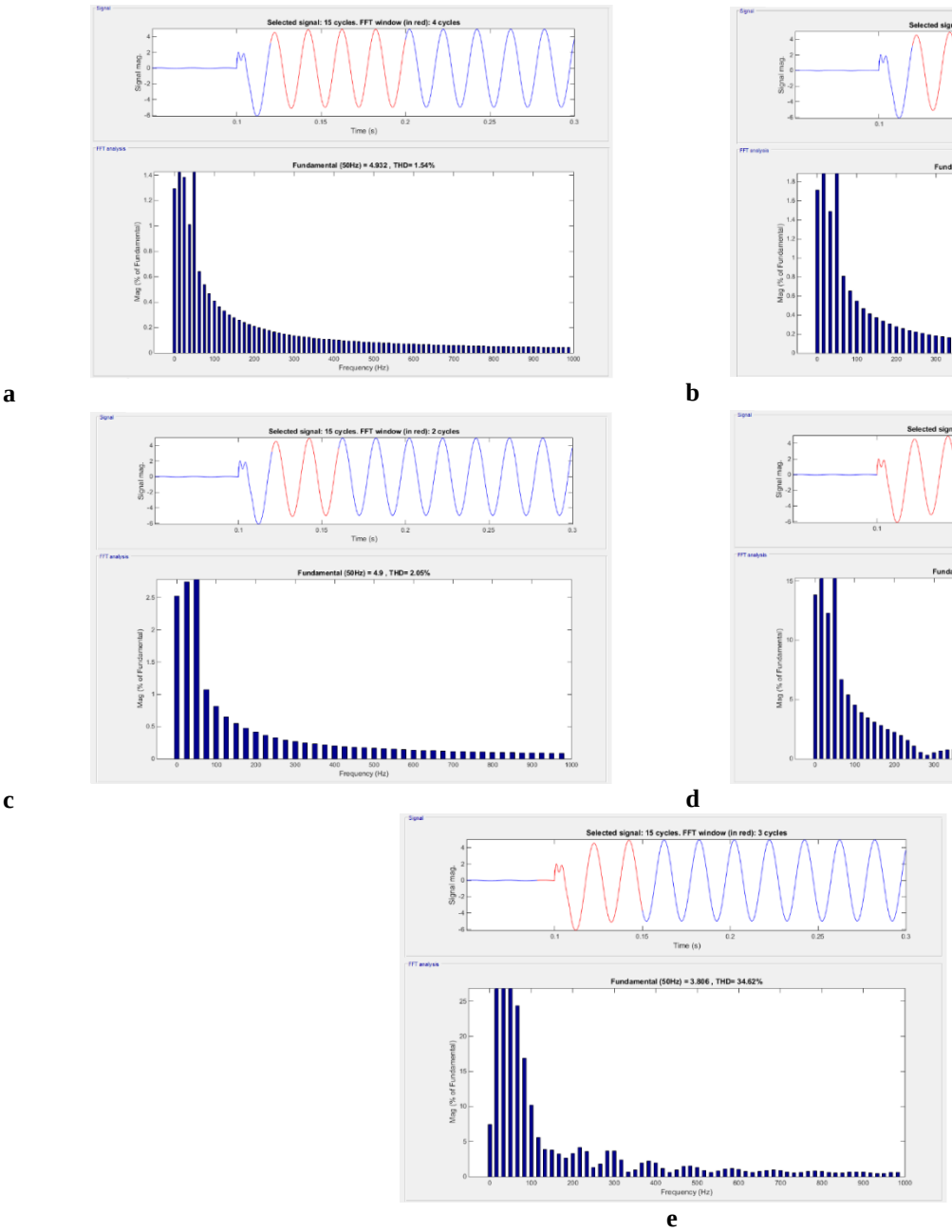

Figure 7: FFT faulty phase current analysis during a continuous fault (a) case of 4 cycles, starting time 0.12s (b) case of 3 cycles, starting time 0.12s (c) case of 2 cycles, starting time 0.12s (d) case of 3 cycles, starting time 0.1s (e) case of 3 cycles, starting time 0.09s.

Table 6. represents the THD compression for all cases done in this work via the faulty phase distortion.

Table 5: Phase 1 current THD values.

Starting time	With fault					Without fault				
	1	2	3	4	5	1	2	3	4	5
0.12	2.36	2.05	1.76	1.54	1.39	0.15	0.12	0.10	0.09	0.08
0.1	19.79	16.21	13.52	11.78	10.56					
0.09	123.75	46.51	34.62	29.03	25.54					
0.075	0.07	86.56	55.25	44.20	38					
0.0501	0.15	0.12	245.49	96.28	72.13					

It can be noticed from the figures and tables, that there is a high level of distortion in the signals for all cases during the fault. Overall, the three-cycle analysis has a considerable distortion compared to the other cycles. Also, it can be noted that the distortion in the current signals is higher than the voltage

signals, even in the healthy phase. There are also some interesting values, such as the maximum current distortion is 245.49%, minimum current distortion is 0.0, maximum voltage distortion is 3.75, and minimum voltage distortion is 0.01. It can be noted that there are some specific values of THD closed to zero, even at the faulty phase. Those values appeared because the starting and ending analysis period is before the fault time, especially in one and two cycles. While three, four, and five cycles analysis have the highest distortion values.

These results could lead us to discover the fault even though the fault current is not much higher than the rated current. Distortion sensors for both currents and voltages during high currents may lead to earlier fault detection. As well as selecting three cycles, there will be an appropriate change to detect the single line to ground fault.

Conclusion

With any part of the power system, underground cable lines are highly affected by abnormal conditions or faults. This study starts with a thorough analysis of a ground fault condition. From a detailed fault, distribution lines distribute a huge amount of power over several distances. This study presents the desired capacitance of the phase conductors to the ground for cables used in the Azadi substation located in the Kurdistan area of Iraq. The simulation findings have demonstrated that high-frequency harmonics may result in the generation of significant distortion voltage and current in the course of a single line to ground fault. This research can be expanded upon in the future to examine the FFT for other kinds of faults, such as L-L-G and L-L faults. Also, it is possible to check for defects that resolve quickly and do not affect stability.

Conflict of interests

None

Author contribution

Conceptualization, Kamal Sheikh Younis; Methodology, Azad Hussein Zubair; Writing—original draft, Azad Hussein Zubair; Writing—review & editing, Kamal Sheikh Younis.

Funding details

This research received no external funding.

References

1. B. Liu, H. Ma, H. Xu, P. J. C. J. o. P. Ju, and E. Systems, "Single-phase-to-ground fault detection with distributed parameters analysis in non-direct grounded systems," *chines society of electrical engineering*, vol. 5, no. 1, pp. 139-147, 2019.
2. Y. Wang *et al.*, "A faulty line detection method for single phase-to-ground fault in resonant grounding system with CTs reversely connected," *International Journal of Electrical power & Energy Systems*, vol. 147, p. 108873, 2023.
3. K. Sagastabeitia, I. Zamora, A. Mazon, Z. Aginako, G. J. I. G. Buigues, Transmission, and Distribution, "Low-current fault detection in high impedance grounded distribution networks, using residual variations of asymmetries," *IET Generation,Transmission and Distribution*, vol. 6, no. 12, pp. 1252-1261, 2012.
4. J. Sun, L. Zhang, M. Chen, Z. Zhao, L. Zhang, and W. Yang, "Feeder Selection Method of Single-Phase High Impedance Grounding Fault in SRGS," in *2021 6th International Conference on Smart Grid and Electrical Automation (ICSGEA)*, 2021, pp. 112-116: IEEE.
5. T.-C. Yu, "Full frequency-dependent modeling of underground cables for electromagnetic transient analysis," University of British Columbia, 2001.
6. R. Ć. U. Č. I. Ć. Vitomir, K. Marijana, and Ž. Ć. Đ. Urovi, "Neutral Point Concept in Distribution Networks," Neutral Point Concept Distrib. Networks, vol. 28, no. 2, pp. 77–89, 2008.
7. V. Mane, P. Mansawale, S. Yawale, and A. Deshmukh, "Cable Fault Detection Methods: A Review," *Int. J. Res. Eng. Sci. Manag.*, vol. 5, no. 6, pp. 2581–5792, 2022.
8. R. N. Mahanty and P. B. D. Gupta, "A fuzzy logic based fault classification approach using current samples only," *Electr. Power Syst. Res.*, vol. 77, no. 5–6, pp. 501–507, 2007.
9. V. Ashok, K. G. V. S. Bangarraju, and V. V. N. Murthy, "Identification and Classification of Transmission Line Faults Using Wavelet Analysis," *ITSI Trans. Electr. Electron. Eng.*, vol. 1, no. 1, pp. 117–122, 2013.
10. S. Dileep, A., Kumar, S., & Raghunath, "Discrimination of Faults and Their Location Identification on a High Voltage Transmission Lines Using the Discrete Wavelet Transform," *Int. J. Educ. Appl. Res.*, vol. 0033, pp. 107–111, 2014.
11. J. Chen, H. Li, C. Deng, and G. Wang, "Detection of Single-Phase to Ground Faults in Low-Resistance Grounded MV Systems," *IEEE Trans. Power Deliv.*, vol. 36, no. 3, pp. 1499–1508, 2021.
12. A. Prasad, J. Belwin Edward, and K. Ravi, "A review on fault classification methodologies in power transmission systems: Part—I," *J. Electron. Syst. Inf. Technol.*, vol. 5, no. 1, pp. 48–60, 2018.
13. V. Komen and R. Cucic, "Fault resistances in medium voltage distribution networks," in *Annals of DAAAM and Proceedings of the International DAAAM Symposium*, 2007, pp. 379–380.
14. A. Prasad, J. B. Edward, C. S. Roy, G. Divyansh, and A. Kumar, "Classification of faults in power transmission lines using Fuzzy-Logic technique," *Indian J. Sci. Technol.*, vol. 8, no. 30, pp. 1–6, 2015.
15. Andrija Krtalić, Vanja Miljković, Dubravko Gajski , Ivan Racetin, "Spatial Distortion Assessments of a Low-Cost Laboratory and Field Hyperspectral Imaging System," *Sensors*, vol 19, no. 19,P 4267, 2019.
16. Saeed and K. Sheikhyounis, "Modeling Features of a Single Phase-to-Earth Fault in a Medium Voltage Overhead Transmission Line," *UKH J. Sci. Eng.*, vol. 4, no. 2, pp. 127–138, 2020.